ELSEVIER

Chemical Engineering Journal 125 (2007) 187–192

Chemical Engineering Journal

www.elsevier.com/locate/cej

Study on a new structure of the separator plate assembly for molten carbonate fuel cell (MCFC) stacks

Li Zhou *, Huaxin Lin, Baolian Yi, Huamin Zhang

Dalian Institute of Chemical Physics, Chinese Academy of Sciences, Dalian 116023, China

Abstract

A new structure of separator plate assembly (SPA), which consisted of a separator plate, flow field plates, perforated plates, frame plates and seal gaskets, was developed for a molten carbonate fuel cell (MCFC) in this study. In this structure, the separator plate, flow field plates and perforated plates were hard-contacted (directly contacted each other); meanwhile the frame plates and the separator plates were bound with the inorganic seal gaskets. SPA and electrodes could be combined together to form a unit of electrode-SPA. The new structure SPA promoted the smooth volatilizing and complete burning of the organic compounds in the matrix. It was effective and reliable to press the stack with a suitable stacking pressure. It was facile and simple to assemble a stack by using electrode-SPA. With the electrode-SPAs, two MCFC stacks were assembled in co-flow and counter-flow, respectively. The performance of Stack B in counter-flow was higher than that of Stack A in co-flow at the same current density. The more uniform temperature distribution and current density distribution in Stack B were responsible for its higher performance.

Keywords: Molten carbonate fuel cell (MCFC); Separator plate assembly (SPA); Stack; Structure

1. Introduction

A fuel cell is an electrochemical reactor, which can continuously convert the chemical energy of a fuel and an oxidant into electrical energy. High temperature fuel cells (HTFC) have many advantages over low temperature fuel cells, such as high efficiency, no need of noble metals as electrode catalysts, flexible choices of fuels, combined heat and power generation (CHP), and cogeneration with gas turbine (GT) and/or stream turbine (ST) [1–5]. As one of the HTFC, molten carbonate fuel cell (MCFC) has its characteristic of the plastic property of the electrolyte matrix and the elasticity of the metal separator plate which is the main structural support element in the MCFC stack [1]. The stack structure may reduce some stresses, which developed due to non-uniform heating of an MCFC. Therefore, a more important advantage of MCFC is that the cell can be scaled-up to a larger size without causing any excessive mechanical stress [1].

In general, a separator plate assembly (SPA) consists of a separator plate, two current collectors, and two flow field plates (or corrugated plate) and so on. They are manufactured by pressing, and then welded together by using electrical resistance seam welding [1]. However, this process is limited by the size of the electrical resistance furnace and the pressure of the pressing. In addition, the welding seam could be corroded under the practical operation condition of MCFC. The corrosion could result in the increase of internal resistance (ohmic drop) and the gas leakage in the stack, thus leading to the performance deterioration.

Up to now, wet-seal of the MCFC is the only practical way to achieve gas tightness when the cell chamber is made of metal [1]. The electrolyte matrix can serve as an edge seal between two SPAs to prevent gas leakage. Wet-seal is also used in the external-manifolded stack widely.

In this study, the components of SPA were machined, and wet-seal was not only served as an edge seal between two SPAs through the sandwiched matrix, but also used in SPA by binding its frame plate and separator plate with inorganic seal gasket. In SPA, the flow field plate, the perforated plate, and separator plate were hard-contacted together as an electronic conductor. The adopted serpentine flow field plate favored more uniform distribution of gas concentrations during sintering matrix and the operation of the stack, avoiding dead zone and shorting pass of gas transportation. As mentioned above, wet-seal was adopted for preparing this new structure of SPA instead of electrical resistance seam welding, so there were no troubles of corrosion on welding seam, thus the performance of the stack could be promoted and stable.

* Corresponding author. Tel.: +86 411 84379103; fax: +86 411 84684839.
E-mail address: zhouli@dicp.cn (L. Zhou).

1385-8947/$ – see front matter © 2006 Elsevier B.V. All rights reserved.
doi:10.1016/j.cej.2006.10.013

Two internal-manifolded MCFC stacks in co-flow and counter-flow were assembled with this new structure of SPA. The change of the stacking pressure with the operation temperature and the performance of the stacks were investigated. Some discussions were also given in this study.

2. Experimental

2.1. Preparation of α-$LiAlO_2$ matrix

Home-made coarse and fine α-$LiAlO_2$ powders [6] were mixed with polyvinyl butyral (PVB) binder and organic additives, such as solvent, plasticizer, dispersant, and anti-bubbling agent. The mixture was ball-milled sufficiently into a paste for 100–120 h. Then the matrices were prepared by tape cast method [6]. Finally they were dried and thermally pressed into the cell matrices. The average thickness of the matrices was 0.7 mm.

2.2. Preparation of SPA

The geometric parameters and materials of the components in the stack of MCFC were listed in Table 1. An electrode-SPA consisted of cathode, cathode frame plate, cathode gasket, cathode perforated plate, cathode flow field plate, separator plate, anode flow field plate, anode perforated plate, anode gasket, anode frame plate and anode, and they were arranged in series as shown in Fig. 1, hereinto the frame plates were placed outside the flow field plate and the perforated plate. The separator plate, flow field plate and perforated plate were hard-contacted (directly contacted each other) to act as electronic conductor. The frame plate and separator plate were bound together with inorganic seal gasket whose shape was the same as that of the frame plate, and were wet-sealed during operation of the stack. The anode and the cathode were jointed to anode perforated plate and cathode perforated plate, respectively. Thus, they were combined into an electrode-SPA, and it was convenient and simple to assemble the stack.

Table 1
Geometric parameters and materials of the components in the stack of MCFC[a]

Component	Thickness (mm)	Area (cm^2)	Materials
Separator plate	1	374.9	SS316L
Perforated plate	1	226	SS316L
Cathode flow field plate	2	226	SS316L
Anode flow field plate	1	226	SS316L
Cathode frame plate	3	28.4 × 13.2 (outside)/20.2 × 11.2 (inside)	SS316L
Anode frame plate	2	28.4 × 13.2 (outside)/20.2 × 11.2 (inside)	SS316L
Cathode gasket	0.3–0.4	28.4 × 13.2 (outside)/20.2 × 11.2 (inside)	α-$LiAlO_2$
Anode gasket	0.4–0.5	28.4 × 13.2 (outside)/20.2 × 11.2 (inside)	α-$LiAlO_2$
Cathode	0.4	226	Ni
Anode	0.4	226	Ni-Cr
Matrix	0.7	374.9	α-$LiAlO_2$

[a] The components in anode and cathode chambers were electroplated with nickel and silver, respectively, and the wet-seal areas of the frame plates and separator plates were coated with aluminum.

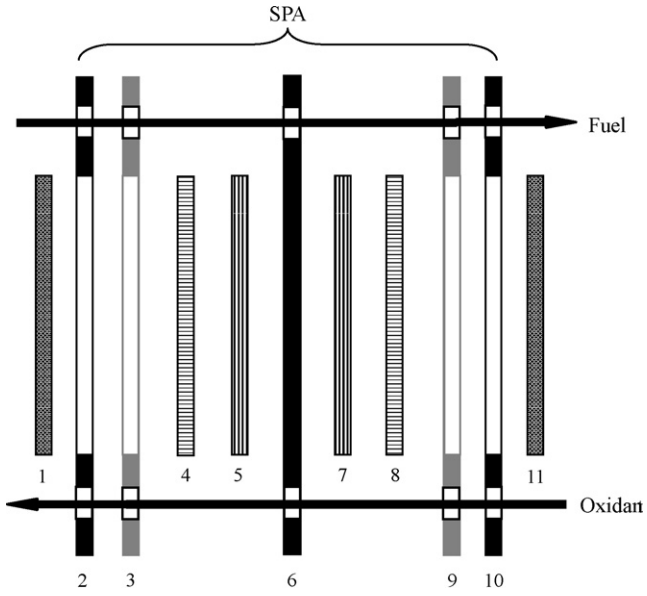

Fig. 1. Structure scheme of electrode-SPA. 1: Cathode; 2: cathode frame plate; 3: cathode gasket; 4: cathode perforated plate; 5: cathode flow field plate; 6: separate plate; 7: anode flow field plate; 8: anode perforated plate; 9: anode gasket; 10: anode frame plate; 11: anode.

Both the flow field plate and perforated plate were combined to guide reactants and products to flow in the anode and the cathode chamber, in which the flow field plate guided the flow in the direction paralleled to the electrode plane and the perforated plate guided the flow in the direction perpendicular to the electrode plane. The adopted serpentine flow field plate favored more uniform distribution of gas concentrations during sintering matrix and the operation of the stack, avoiding dead zone and shorting pass of gas transportation.

2.3. Assembly, starting-up and operation of the MCFC stacks

The structure of the MCFC stack was shown schematically in Fig. 2. Carbonate salts (0.62 Li_2CO_3 + 0.38 K_2CO_3) electrolyte was pre-stored in the cathode and the anode chamber, *i.e.* in the gaps of the perforated plates and flow field plates. The two stacks were assembled in different gas flow type of co-flow and counter-flow, respectively, and each stack consisted of 26 cells. They were placed side by side between two same compression plates.

The stacks were heated up slowly at the rate of 0.03 °C min^{-1}. At the same time, oxygen gas was introduced into the cathode and the anode chamber. Keeping the temperature at 650 °C, gas tightness including gas cross-over across the matrix and leakage in the stack were checked with N_2. The $O_2 + CO_2$ ($O_2/CO_2 = 40/60$) and $H_2 + CO_2$ ($H_2/CO_2 = 80/20$) mixture gases as oxidant and fuel were introduced into the cathode and

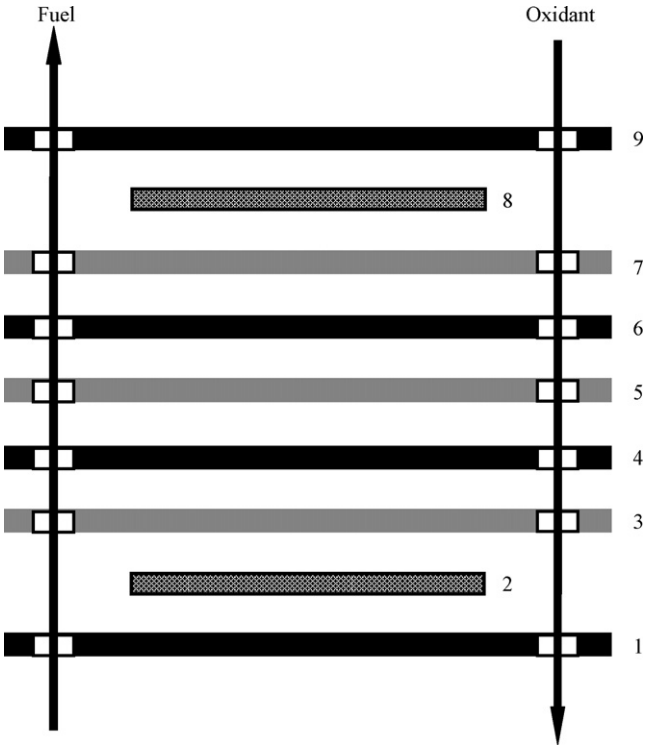

Fig. 2. Structure scheme of MCFC stack. 1: Anode end-plate; 2: anode; 3, 7: matrix; 5: repeating element – matrix; 4: electrode-SPA; 6: repeating element – electrode-SPA; 8: cathode; 9: cathode end-plate.

the anode chambers, respectively. When open circuit potential of each cell was higher than 1.1 V, the stack performance was measured.

3. Results and discussion

3.1. Sintering matrix during starting-up

The stacks were heated slowly at the rate of 0.03 °C min^{-1} and at the same time oxygen gas was introduced into the stack. Oxygen gas passed through the oxidant and fuel internally manifolding to the cathode and anode chamber, then it passed through serpentine flow field plate and perforated plate of SPA, and reached the surface of the matrix through porous electrodes. Oxygen distribution was more uniform because of the shape of the serpentine flow field plate, thus leading to more uniform distribution of temperature and avoiding intense local heating in the cell. With the elevating of temperature in the stack, the organic additives volatilized from the matrix and PVB burnt in oxygen gas [7]. On the contrary, the volatilized and burnt products of the organic compounds were expelled from the cathode and the anode chamber. After the volatilizing and burning out of the organic compounds, the matrix became a porous ceramic plate. When the temperature was about 500 °C, the electrolyte pre-stored in the chambers began to melt gradually and was impregnated into the porous ceramic matrix by capillary force. Finally, the matrix was full of the electrolyte and became a sealed and ionic conductor layer, in which porous ceramic matrix was the support-frame and molten carbonate anion (CO_3^{2-}) was the carrier ion. In the meantime, the electrodes were partially filled with the molten carbonate salts.

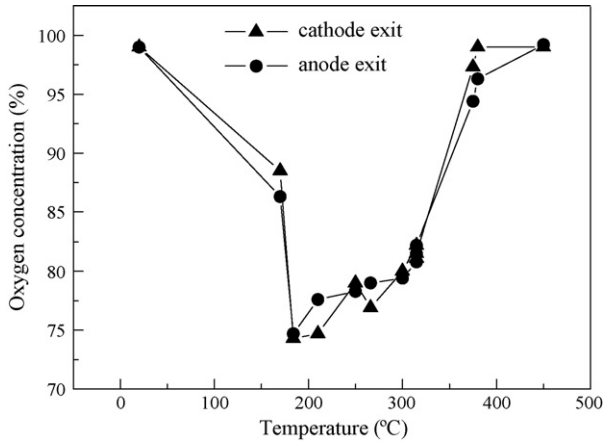

Fig. 3. Oxygen concentrations at the exits of cathode and anode in the two MCFC stacks changed with elevating temperature.

Oxygen concentrations at the exits of the cathode and anode chambers were measured by an oxygen sensor, and they changed with elevating temperature as shown in Fig. 3. Two curves of them were alike. When the temperature elevated from room temperature to 150 °C, oxygen concentration (99%) decreased due to the volatilization of the organic compounds with lower boiling point (BP). When the temperature elevated from 150 to 180 °C, it decreased significantly because of the volatilization of the organic compounds with higher BP, and at 180 °C, PVB started to burn [8] and oxygen concentration decreased to the lowest, 74.3%. In the temperature range 180–320 °C, oxygen concentration increased slowly due to the decrease of PVB remained in the matrix. In the temperature range 320–400 °C, PVB burning was going to be finished, both the kinds and the quantities of the burnt products decreased [8], and the oxygen concentration increased over 90%. When temperature elevated from 400 to 450 °C, oxygen concentration increased to the original value 99%, because only a small amount of tar (burning residual) was burnt at the end of the burning process.

Thermal gravimetric curve for the α-$LiAlO_2$ matrix out-of-cell was shown in Fig. 4. The rates of weight loss in the matrix were higher in "BC" and "CD" temperature range, which were

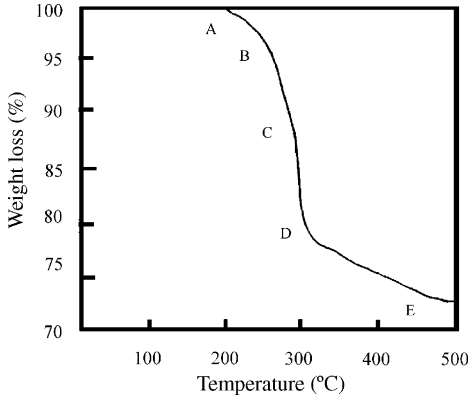

Fig. 4. Thermo gravimetric curve for the α-$LiAlO_2$ matrix.

corresponding to the volatilization of the organic compounds with lower BP, and the volatilization of those with higher BP and burning of PVB in the matrix, respectively. Compared with Fig. 3, it was proved that the adopted serpentine flow field plate favored smooth gas transportation and more uniform distribution of gas concentration in the SPA, resulting in complete burning of organic compounds in the matrix.

3.2. Change of the stacking pressure

The contact between the components in SPA directly affected the electronic conductivity and the IR drop (ohmic drop). In order to increase the ability of gas tightness and to decrease the contact resistance between the components in the stacks, especially in the hard-contacted SPA, the stacking pressure should be sufficient and suitable.

The change of stacking pressure was measured by the pressure transducer during the starting-up and operation of the stacks. The tested two stacks were placed side by side and both share the same compression plates. The original stacking pressure was 7.5 MPa for the two stacks with the total sectional area of 749.8 cm^2 (the sectional area per stack was 374.9 cm^2 which was the same as that of a separator plate/matrix), which was extrapolated from the previous study [9]. If the stacking pressure was too high, the stack would be pressed densely, fewer gas channels would form on the seal gasket area, and the organic compounds would not volatilize smoothly and burn completely [7] in the burning process of the matrix, in which the organic compounds would carbonize, further resulting in short circuit in the stack. If the stacking pressure was too low, the components in the stack would contact insufficiently each other, thus the performance would decline greatly due to the higher ohmic resistance between the components. At the same time, big leakage of the gases would occur along the seal surface in the stack. Therefore, a suitable stacking pressure adopted for the first starting-up of the stack was necessary.

With elevating operation temperature, the stacking pressure dropped. As shown in Fig. 5, it dropped distinctly from room temperature to 200 °C, and became slightly fluctuation from 200 to 490 °C and dropped abruptly from 490 to 650 °C. When the operation temperature was kept at 650 °C, the stacking pressure continued dropping for 48 h. Finally it stayed at 2.0 MPa. The change of stacking pressure was resulted from synergistic effects of more factors presented as follows.

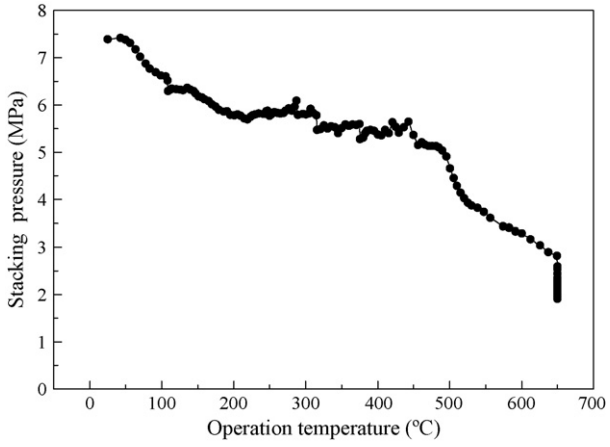

Fig. 5. The change of stacking pressure with operation temperature.

During the elevating of operation temperature, the stacking pressure dropped from room temperature to 200 °C due to the matrix softened by heat. From 200 to 490 °C, the volatilizing and burning of organic compounds, the thermal expanding of metal component and the shrinkage of matrix coexisted simultaneously. As the stacking pressure dropped the extent of the shrinkage of the matrix was more than that of the expanding of metal components.

The shrinkage of the matrix volume might be mainly caused by the volatilizing and burning out of the organic compounds under the stacking pressure. The dropping of the stacking pressure from 200 to 490 °C was mainly caused by this shrinkage. However, the sudden drop from 490 to 650 °C might be caused by the electrolyte melting and matrix and seals softening after the electrolyte impregnation, as well as the flow field plates and the porous electrodes deformation under the stacking pressure.

Besides the decrease of contact resistance, another important function of the suitable stacking pressure was to produce gas tightness in the stack, which was necessary for the overall operation process, especially for the starting-up. The original stacking pressure before the starting-up was suitable to prevent the matrix and gasket from being cracked or from being deformed and slipped; and the final stacking pressure should meet the requirement for the gas tightness under the operation condition, because it dropped greatly with the elevating of the temperature as mentioned above. The final stacking pressure of 2.0 MPa was high enough to keep up gas tightness in the stack, because there were two wet-seals between one separate plate and two frame plates in every SPA, and there was one wet-seal between every two neighbor SPAs.

3.3. Effect of flow type on stack performance

With the electrode-SPA, two MCFC stacks were assembled in different flow types – co-flow and counter-flow, respectively. $O_2 + CO_2$ ($O_2/CO_2 = 40/60$) and $H_2 + CO_2$ ($H_2/CO_2 = 80/20$) mixture gases were fed into the cathode and the anode chambers, respectively. The performances of the stacks were measured under the following operation conditions: temperature 650 °C and gas pressure 0.1 and 0.5 MPa, while keeping the utilization of fuel and oxidant at 20%.

Fuel and oxidant were fed into inlets at the top end plate of Stack A, and flew in each cell in the flow type of co-flow. The performance of the Stack A was shown in Fig. 6(a). The performance gain of the pressurized stack is in the two parts with increasing pressure of reaction gas, the first part is reversible thermodynamic amount which is the gain of equilibrium voltage according to the Nernst equation, the second one is irreversible kinetic amount due to decreasing all polarizations with increasing pressure of reaction gas, that is ascribed to the increase of solubility of reaction gas in the melt and the acceleration of electrode kinetics. In general, the later is more than two times of the former at higher current density.

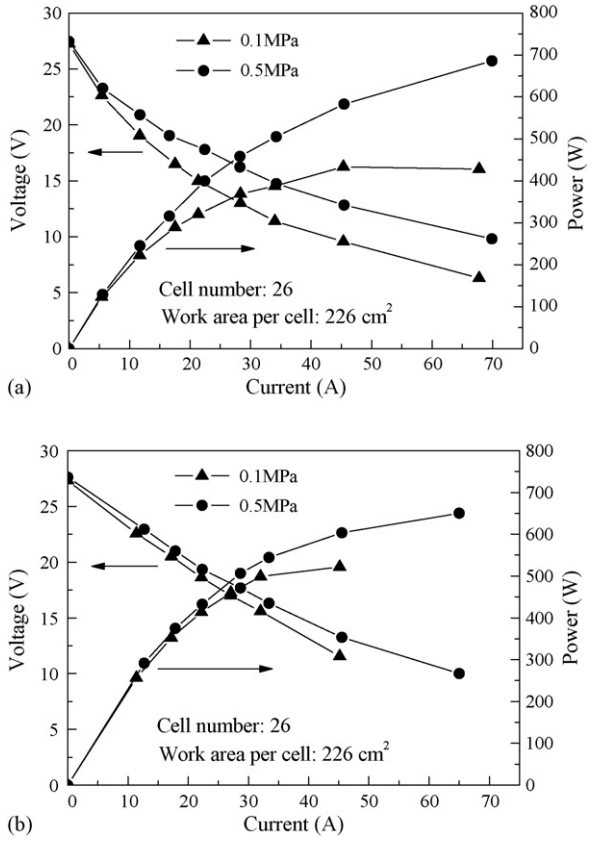

Fig. 6. (a) Performance curves of the MCFC stack in co-flow configuration. (b) Performance curves of the MCFC stack in counter-flow configuration.

In Stack B, fuel and oxidant were fed into the inlets at the bottom end plate and at the top end plate, respectively. They flew in each cell in the flow type of counter-flow. The performance of Stack B was shown in Fig. 6(b). The terminal voltage and output power of Stack B were higher than those of Stack A at the same current density. The higher performance might be caused by the more uniform distribution of the temperature and gas concentrations [10–13] in Stack B compared with those in Stack A.

Although the temperatures of fuel and oxidant at all the inlets were 510 °C at which they were preheated by the exchangers and the heaters, the non-uniform distribution of the temperature still existed within the same cell and between the cells in the same stack. The non-uniform distribution was caused by the different gas concentrations within Stack A especially when the stack was loaded. When the stack was operated in co-flow, both reactant concentrations at the inlets were the highest and decreased along the same flow direction; meanwhile the product concentrations increased and became the highest at the outlets. The temperature was lower at the inlets and increased along the same flow direction due to the heat produced from electrochemical reactions and polarizations [10,12,14,15].

When the stack was operated in the flow type of counter-flow of fuel gas and oxidant, along the fuel flow direction, fuel concentration decreased but oxidant concentration increased in the same cell [15,16]. The consumption of fuel and oxidant seemed to be symmetric along their respective flow direction. Current density distribution seemed to be more uniform, and temperature distribution was less affected by gas concentrations distribution and by current density distribution. They were more uniform in Stack B than those in Stack A. Therefore, the performance of Stack B was higher than that of Stack A at the same current density.

The more uniform current density and temperature distribution in Stack B were caused not only by the counter-flow of the fuel and oxidant but also by the serpentine flow field in SPA presented above.

4. Conclusions

The components of SPA were machined and the wet-seal was used in SPA by binding the frame plate and separator plate with the inorganic seal gasket. In the SPA, the flow field plate, the perforated plate, and the separator plate were hard-contacted together as an electronic conductor. SPA was combined with the anode and the cathode to form an electrode-SPA. The new structure of SPA promoted the smooth volatilizing and complete burning of the organic compounds in the matrix. It was effective and reliable to press the stack with the suitable stacking pressure. During the starting-up of the stacks, the stacking pressure dropped with elevating temperature. The shrinkage of the matrix was the dominant factor in the dropping of the stacking pressure. Two MCFC stacks were assembled in different flow types of co-flow and counter-flow by using electrode-SPAs. The stack potential and output power of Stack B in counter-flow were higher than those of Stack A in co-flow at the same current density. The more uniform temperature distribution and current density distribution in Stack B were responsible for its higher performance.

Acknowledgements

The authors are thankful for the financial supports from Chinese Ministry of Science and Technology and Chinese Academy of Sciences.

References

[1] L.J.M.J. Blomen, M.N. Mugerwa, Fuel Cell Systems, Plenum Press, New York, 1993, pp. 399–414.
[2] T. Kivisaari, P. Björnbom, C. Sylwan, B. Jacquinot, D. Jansen, A. Groot, The feasibility of a coal gasifier combined with a high-temperature fuel cell, Chem. Eng. J. 100 (2004) 167–180.
[3] M.C. Williams, J.P. Strakey, S.C. Singhal, U.S. distributed generation fuel cell program, J. Power Sources 131 (2004) 79–85.
[4] P. Lunghi, R. Bove, U. Desideri, Analysis and optimization of hybrid MCFC gas turbines plants, J. Power Sources 118 (2003) 108–117.
[5] Y. Yi, A.D. Rao, J. Brouwer, G.S. Samuelsen, Analysis and optimization of a solid oxide fuel cell and intercooled gas turbine (SOFC–ICGT) hybrid cycle, J. Power Sources 132 (2004) 77–85.
[6] H.X. Lin, B.L. Yi, L. Zhou, C.Q. He, L.Y. Kong, E.J. Zhang, A study on the performance of matrix prepared by tape cast and its molten carbonate fuel cells (MCFCs), Electrochemistry (China) 6 (4) (2000) 109–119.
[7] H.X. Lin, L. Zhou, C.Q. He, L.Y. Kong, E.J. Zhang, B.L. Yi, A study on the dependence of the micro-pore configurations on the volatilization and the burn processes of the organic compounds in the matrix of molten carbonate fuel cells, Electrochim. Acta 47 (2002) 1451–1459.

[8] J.J. Seo, S.T. Kuk, K. Kim, Thermal decomposition of PVB (polyvinyl butyral) binder in the matrix and electrolyte of molten carbonate fuel cells, J. Power Sources 69 (1997) 61–68.
[9] H.X. Lin, B.L. Yi, L.Y. Kong, E.J. Zhang, L. Zhou, F.X. Wang, Study on preparation of coarse and fine γ-$LiAlO_2$ mixed power used for MCFC matrix, Electrochemistry (China) 6 (1) (2000) 57–64.
[10] J.H. Koh, H.K. Seo, Y.S. Yoo, H.C. Lim, Consideration of numerical simulation parameters and heat transfer models for a molten carbonate fuel cell stack, Chem. Eng. J. 87 (2002) 367–379.
[11] J.H. Koh, B.S. Kang, H.C. Lim, Effect of various stack parameters on temperature rise in molten carbonate fuel cell stack operation, J. Power Sources 91 (2000) 161–171.
[12] F. Stand.aert, K. Hemmes, N. Woudstra, Analytical fuel cell modeling: non-isothermal fuel cells, J. Power Sources 70 (1998) 181–199.
[13] H. Hirata, M. Hori, Gas-flow uniformity and cell performance in a molten carbonate fuel cell stack, J. Power Sources 63 (1996) 111–120.
[14] R. Fellows, A novel configuration for direct internal reforming stacks, J. Power Sources 71 (1998) 281–287.
[15] F. Yoshiba, N. Ono, Y. Izaki, T. Watanabe, T. Abe, Numerical analyses of the internal conditions of a molten carbonate fuel cell stack: comparison of stack performances for various gas flow types, J. Power Sources 71 (1998) 328–336.
[16] P. Heidebrechta, K. Sundmachera, Molten carbonate fuel cell (MCFC) with internal reforming: model-based analysis of cell dynamics, Chem. Eng. Sci. 58 (2003) 1029–1036.